



OPEN

A new silver coordination polymer based on 4,6-diamino-2-pyrimidinethiol: synthesis, characterization and catalytic application in asymmetric Hantzsch synthesis of polyhydroquinolines

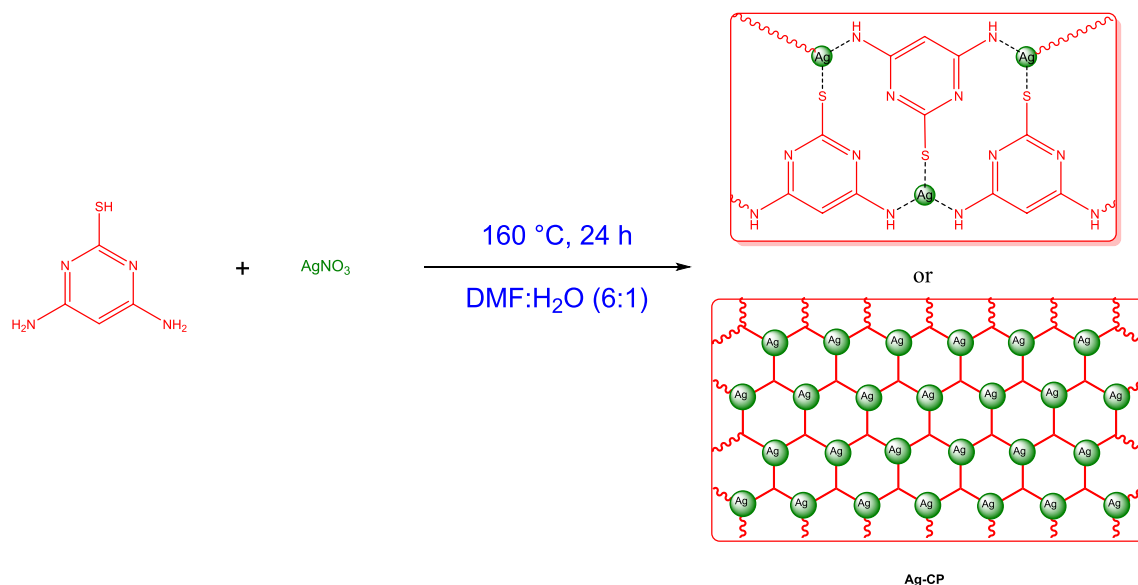
Noorullah Hussain-Khil¹, Arash Ghorbani-Choghamarani²✉ & Masoud Mohammadi¹

A highly efficient and stable heterogeneous coordination polymer (CP) was successfully prepared by hydrothermal combination of silver and 4,6-diamino-2-pyrimidinethiol. The prepared coordination polymer was characterized by FT-IR, XRD, TGA, SEM, EDX, X-ray mapping and Nitrogen adsorption-desorption analysis. The prepared Ag-CP exhibit excellent catalytic activity in multicomponent Hantzsch synthesis of polyhydroquinolines under mild reaction conditions in relatively short reaction times. The heterogeneity of the catalyst was confirmed by the hot filtration test; also, the catalyst was reused for at least four times under the optimized reaction conditions without any significant loss of its catalytic activity.

Several important applications of organosilver compounds in organic chemistry have been recognized for a long time, i.e. applying silver reagents in the several reactions such as cycloaddition reactions, cyclization, coupling reactions and C-H functionalization, carbene, nitrene, silylene-transfer reactions and so on¹⁻⁶. From the environmental and economic points of view, catalytic functional groups transformation technologies signify an important tool for the development of “green chemistry”, which means less waste generation and little energy consumption, as well as high atom economy and environmental friendliness^{7,8}. Accordingly, as a result of their high catalytic performance, many transition metals, especially valuable metals such as ruthenium, platinum, palladium and iridium, are applied in these transformations⁹⁻¹². However, in view of their limited abundance on earth, high prices and toxicity, chemists began to scrutinize new catalyst systems using first and second-row transition metals¹³. Currently, cheap, abundant and low-toxic metals—such as silver—have gained widespread attention of the synthetic community. In this sense, the coordination polymers have caught the attention as catalytic systems for many heterogeneous industrial reactions¹⁴⁻¹⁹. These types of heterogeneous catalysts are attractive due to their structural ordering, large size and volume of pores, and large specific surface area²⁰⁻²³. Furthermore, when compared to conventional mesostructured silica-based supports, the CPs ones have shown much higher activity and selectivity by providing good and regular interaction between metal species and organic reagents^{24,25}. It has been found out that Ag-based CPs show high surface area and, as a result, a large number of reactions happen in presence of Ag-CP as catalyst²⁶⁻²⁹. Actually, in a number of cases, such reactions occur more proficiently and with more selectivity, as compared to the reactions carried out in presence of other types of heterogeneous nanomaterials. Such reactions are simple to handle, can diminish pollution, are comparatively cheaper in industrial sector.

Moreover, multicomponent reactions (MCRs) are synthetic protocols which are able to join three or more substrates together in a highly regio- and stereoselective manner in order to deliver the structurally complex

¹Department of Chemistry, Faculty of Science, Ilam University, Ilam, Iran. ²Department of Organic Chemistry, Bu-Ali Sina University, Hamedan 6517838683, Iran. ✉email: a.ghorbani@basu.ac.ir



Scheme 1. The synthesis of Ag-CP.

organic molecules^{30–32}. Accordingly, it is worth mentioning that they have been remarkably applied in all fields of organic synthesis^{7,13,33–36}. But, regarding the one pot synthesis, they give yield in a highly stereoselective manner which is useful for the organic transformations^{37–39}. MCRs have remarkable benefits in terms of simplicity and synthetic efficiency over formal chemical reactions and show high atom economy and high selectivity^{40–43}. Therefore, the use of MCRs as well as domino reaction sequences has significantly increased for a large number of products⁴⁴. Nowadays, we are fascinated in developing a facile MCR procedure to synthesize polyhydroquinolines, in view of their interesting applications in medicinal and materials chemistry. The synthesis of polyhydroquinoline derivatives can be regarded as an example of the Hantzsch dihydropyridine (Pyridine) synthetic method¹³. Polyhydroquinolines have fascinated much interest because of their diverse pharmacological and therapeutic properties¹³. Most of the reported methods to synthesize polyhydroquinolines possess some specific drawbacks such as low yield, harsh reaction condition and use of volatile organic solvent^{7,45–47}. The use of a variety of homogeneous and heterogeneous catalysts has been previously reported to synthesize various densely substituted polyhydroquinolines via traditional organic synthesis or MCR synthesis^{37,48–53}. However, we have developed a new protocol with environmentally benign condition and also with the high catalytic efficiency of the novel Ag-CP by the condensation reaction of the substituted aromatic aldehydes, ethyl acetoacetate, dimedone and ammonium acetate with excellent yields. Moreover, this catalyst can be easily separated from the reaction solution and would also exhibit an enduring catalytic activity in the long-term reaction.

Experimental

Preparation of Ag-CP. A solution of 4,6-diamino-2-pyrimidinethiol (1 mmol) in water (2 mL) was prepared and, then, added to a solution of AgNO₃ (2 mmol) in DMF (12 mL). The obtained mixture was stirred under darkness at 80 °C for 20 min. Afterwards, the mixture was kept in an autoclave at 160 °C for 24 h (Scheme 1). In the next step, the obtained powder from the autoclave was cooled down and washed with ethyl acetate. Subsequently, the obtained Ag-CP black powder was sonicated for 20 min, dried in room temperature and, finally, stored in a dark brown bottle.

General procedure for the catalytic synthesis of polyhydroquinolines. A mixture of aromatic aldehydes (1.0 mmol), ethyl acetoacetate (1 mmol), dimedone (1 mmol), NH₄OAc (1.2 mmol) and Ag-CP (8 mg) was stirred in EtOH under reflux conditions for the required time. The progress of reaction was monitored by TLC. After completion of the reaction, the mixture was cooled down to room temperature. Afterwards, the catalyst was separated using simple filtration and, then, washed by hot ethyl acetate. Finally, the solvent was evaporated and the pure polyhydroquinoline products was obtained through recrystallization in ethanol.

Selected spectral data. *Ethyl-4-(4-methylphenyl)-2,7,7-trimethyl-5-oxo-1,4,5,6,7,8-hexahydroquinoline-3-carboxylate.* ¹H NMR (500 MHz, DMSO): δ (ppm) 0.84 (s, 3H), 1.00 (s, 3H), 1.12 (t, J = 7.2 Hz, 3H), 1.95 (d, J = 16.0 Hz, 1H), 2.14–2.19 (m, 4H), 2.23–2.31 (m, 4H), 2.41 (d, J = 16.8 Hz, 1H), 3.96 (q, J = 7.2 Hz, 2H), 4.80 (s, 1H), 6.99 (d, J = 7.6 Hz, 2H), 7.02 (d, J = 7.6 Hz, 2H), 9.01 (s, 1H); ¹³C NMR (126 MHz, DMSO) δ 194.29, 166.92, 149.40, 144.83, 144.80, 134.57, 128.34, 127.41, 110.11, 103.79, 59.04, 35.42, 32.17, 29.12, 27.05, 20.83, 18.28, 14.20.

Ethyl-4-(3-hydroxyphenyl)-2,7,7-trimethyl-5-oxo-1,4,5,6,7,8-hexahydroquinoline-3-carboxylate. ¹H NMR (500 MHz, DMSO): δ (ppm) 0.87 (s, 3H), 1.00 (s, 3H), 1.16 (t, J = 7.2 Hz, 3H), 1.97 (d, J = 16.0 Hz, 1H), 2.17 (d, J = 16.0 Hz, 1H), 2.27 (m, 4H), 2.40 (d, 1H), 4.00 (m, 2H), 4.79 (s, 1H), 6.47 (d, J = 7.2 Hz, 1H), 6.58–6.63

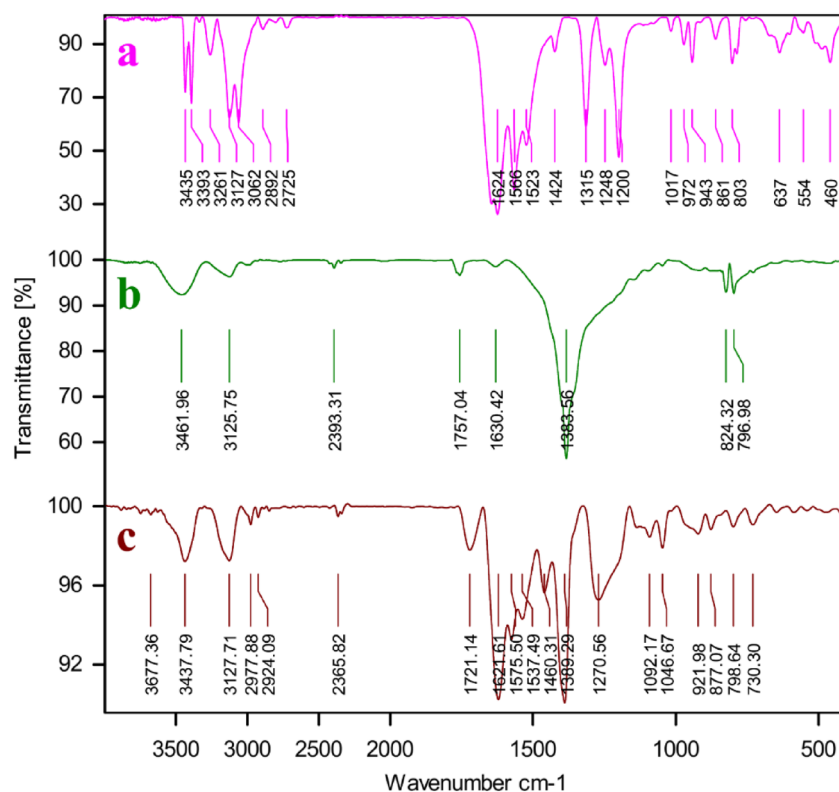


Figure 1. FT-IR Spectrums of (a) 4,6-diamino-2-pyrimidinethiol, (b) Silver nitrate and (c) Ag-CP.

(m, 2H), 6.90–6.96 (m, 1H), 9.01 (s, 1H), 9.07 (s, 1H); ^{13}C NMR (126 MHz, DMSO) δ 194.31, 166.98, 156.86, 149.48, 149.00, 144.76, 128.56, 118.11, 114.69, 114.50, 109.94, 103.65, 59.06, 49.87, 35.64, 32.17, 29.18, 26.58, 18.35, 14.21.

Ethyl-4-(4-chlorophenyl)-2,7,7-trimethyl-5-oxo-1,4,5,6,7,8-hexahydroquinoline-3-carboxylate. ^1H NMR (400 MHz, DMSO-d₆): δ (ppm) 0.82 (s, 3H), 0.99 (s, 3H), 1.10 (t, $J=7.2$ Hz, 3H), 1.98 (d, $J=15.6$ Hz, 1H), 2.18 (d, $J=14.4$ Hz, 1H), 2.26–2.29 (m, 4H), 2.41 (d, $J=17.2$ Hz, 1H), 3.96 (q, $J=6.8$ Hz, 2H), 4.84 (s, 1H), 7.11–7.19 (m, 2H), 7.21–7.29 (m, 2H), 9.11 (s, 1H); ^{13}C NMR (126 MHz, DMSO) δ 194.29, 166.68, 161.23, 149.65, 146.61, 145.47, 130.23, 129.36, 127.72, 109.70, 103.14, 59.14, 50.17, 35.67, 35.60, 32.16, 29.12, 26.45, 18.38, 18.31, 14.15.

Results and discussion

Structural and chemical composition analysis. The FT-IR spectrum of the 4,6-Diamino-2-pyrimidinethiol (Fig. 1a) before of the CPs complexation had absorption bands in the regions of 3339 cm^{-1} and 3435 cm^{-1} respectively, related to the stretching vibration of the N–H bonds of free NH_2 groups. This bands disappeared in the FT-IR spectra of the Ag-CP (Fig. 1c), which is indicative of the fact that the NH_2 groups of 4,6-diamino-2-pyrimidinethiol have been deprotonated and coordinated to the Ag atoms. Moreover, a shift on the bending vibration of NH_2 near 1628 cm^{-1} in the Ag-CP to more higher wavenumbers in comparison to the 4,6-Diamino-2-pyrimidinethiol demonstrates the existence of the metal coordination bonding and confirms the successful complexation of Ag ions with the nitrogen atoms and thiol atoms of ligand. In the curve of the Ag-CP (Fig. 1c), the strong C=C stretching vibration band at 1460 cm^{-1} , and C–N stretch band at 1092 cm^{-1} provide evidences confirming the successful synthesis of Ag-CP. On the basis of the FT-IR, we can also observe that the FT-IR spectrum of Ag-CP obtained from silver nitrate (Fig. 1b) shows sharp characteristic peaks suggesting the high crystalline nature of Ag-CP. On the basis of the FT-IR results Silver ions were coordinated to the amine and thiol functional groups of 4,6-Diamino-2-pyrimidinethiol as a tridentate ligand and confirm the suggested structure in Scheme 1.

The synthesized CPS materials were characterized by PXRD analysis using PW1730 instrument from Philips Company having $\text{CuK}\alpha$ ($\lambda=1.540598\text{ \AA}$) radiation at 40 kV and 30 mA with $2\theta=10^\circ\text{--}80^\circ$. The XRD pattern of Ag-CP is shown in Fig. 2. According to powder PXRD standards (PXRD, Ref. No. 01-087-0718), the crystalline peaks occurring at $2\theta=38.48^\circ$, 44.77° , 64.99° and 77.92° can be attributed to the (111), (200), (220), and (311) crystallographic planes of silver crystals, which are in agreement with the previously reported literatures⁵⁴. The PXRD patterns shown in Fig. 2 confirm the successful coordination of silver ions within the prepared framework. In addition, the (111) Ag diffraction peak with appreciable intensity further confirms the presence of Ag metal in the prepared Ag-CP⁵⁵.

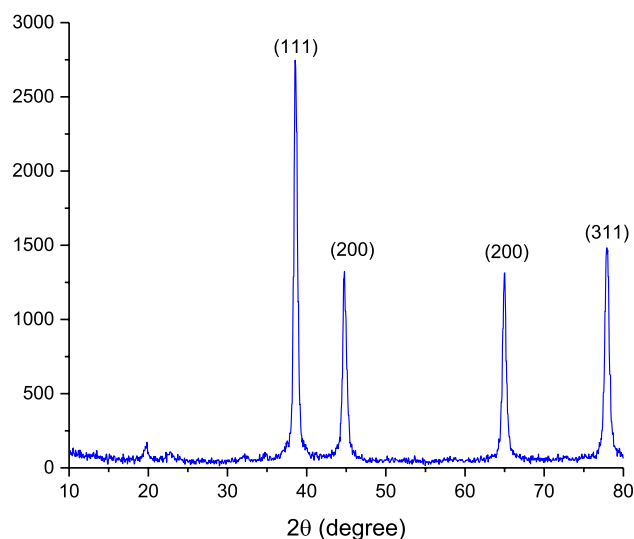


Figure 2. PXRD pattern of Ag-CP.

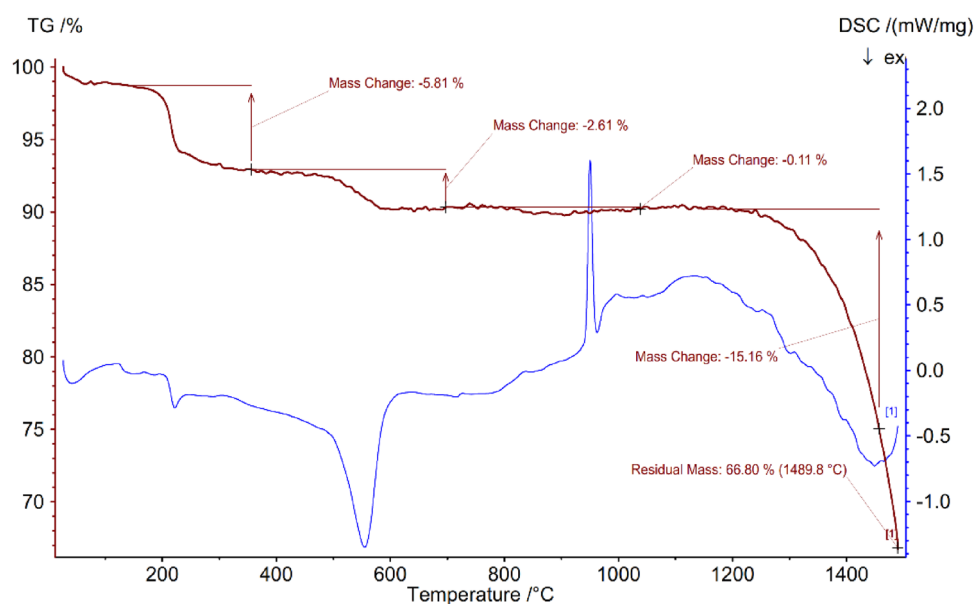


Figure 3. TGA/DSC curves of Ag-CP.

The mass ratios and the thermal stability of Ag-CP were examined by the thermogravimetric analysis (TGA) (Fig. 3). In all of the TGA curve, the weight loss which was occurred below 200 °C was attributed to the release of physically adsorbed moisture and water and organic solvents from the sample⁵⁶. It was at above 200 °C that the framework degradation started. The main weight loss at 250–600 °C was caused by the decomposition of 4,6-Diamino-2-pyrimidinethiol ligand^{57,58}. This result confirms the successful synthesis of Ag-CP, and the fact that the temperature stability of the sample is about 200 °C. The DSC results which support the TGA data, based on weight loss of the sample, approve the range of temperature stability of the sample.

As shown in the Fig. 4, the morphology of the surfaces of the obtained Ag-CP porous material was further characterized by scanning electron microscopy. A closer look at the SEM images of the obtained porous material indicates that the Ag-CP have been formed in uniform nanometer-sized particles.

The EDX spectrum showed that a lot of Ag species was observed on the surface of the obtained Ag-CP porous catalyst in Fig. 5. The presence of C, S and N elements in the Ag-CP was also confirmed by energy dispersive X-ray (EDX) measurements.

The X-ray mapping technique was performed in order to complete the characterization of the Ag-CP elements and how they are distributed in the CPs structure. Figure 4 shows the elemental X-ray mapping of Ag-CP. The uniform distribution of the index elements (C, S, N, and Ag) is observed at the obtained porous material. The

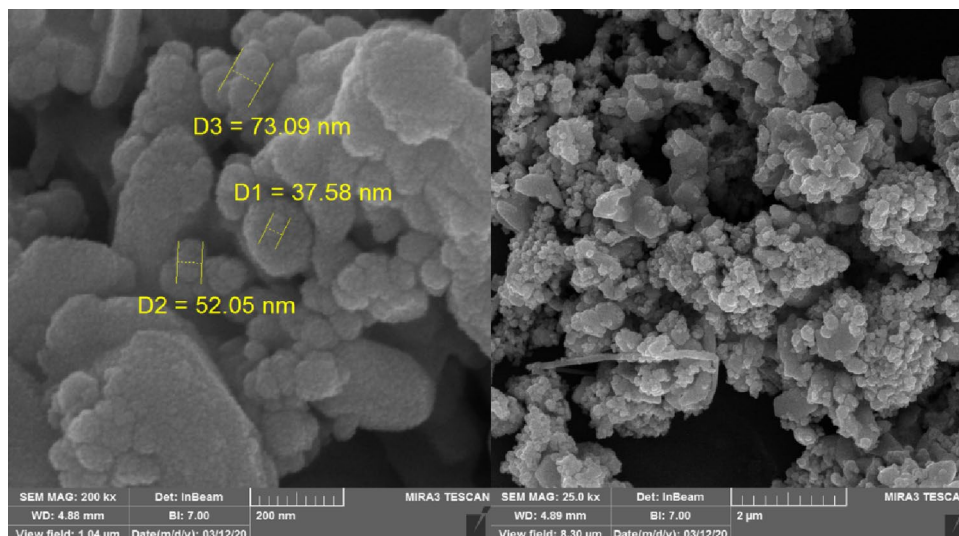


Figure 4. SEM images of Ag-CP.

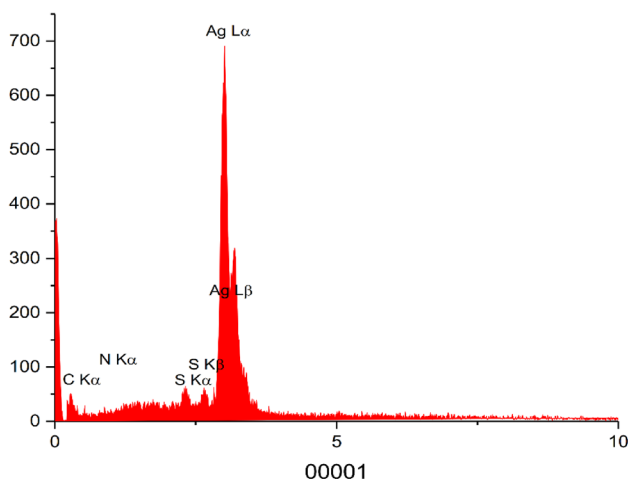


Figure 5. EDX Analysis of Ag-CP.

uniform distribution of C, N and S elements indicated the presence of the 4,6-diamino-2-pyrimidinethiol scaffold, which has been used as a ligand. In addition, the uniform distribution of the Ag element can be seen in the X-ray-mapping images. It can be concluded from the figure that the Ag has evenly coordinated to 4,6-diamino-2-pyrimidinethiol scaffold, and a good catalytic surface has been formed via the uniform incorporation of Ag catalytic species with nitrogen and sulfur groups (Fig. 6).

The surface area and pore size distribution of Ag-CP are studied by BET analysis which exhibits type IV adsorption isotherm according to IUPAC classification. The appeared characteristic hysteresis loop is in good agreement with CPs material (Fig. 7). Regarding the BET analysis, the calculated surface area of Ag-CP is 3.59 m²/g. The pore volumes and pore size distribution of Ag-CP are calculated by BJH analysis and the values are 0.02 cm³ g⁻¹, and 23.45 nm, respectively. Which indicated that the obtained Ag-CP is a mesoporous material. These results are in agreement with the reported coordination compounds in literature^{59,60}.

Catalytic study. After the successful characterization of the synthesized Ag-CP, its catalytic activity was evaluated in multicomponent Hantzsch condensation of polyhydroquinolines under diverse conditions (Table 1). Firstly, the Hantzsch reaction was carried out between *para*-chlorobenzaldehyde and dimedone, ethyl acetoacetate and ammonium acetate as a model reaction. Afterwards, we aimed at investigating the optimum reaction conditions in presence of the newly synthesized Ag-CP catalyst. Table 1 clearly depicts that the reaction progress is highly affected with catalyst loading, solvent and temperature. At the first step, the effect of Ag-CP loading to catalyze the reaction was examined by varying the amount of Ag-CP in the model reaction. It was observed that the yield of the polyhydroquinoline product enhanced with increasing the amount of the catalyst from 1 to 7 mg (Table 1, entries 4–10). The best result in an appropriate time was obtained using 7 mg of the catalyst (Table 1,

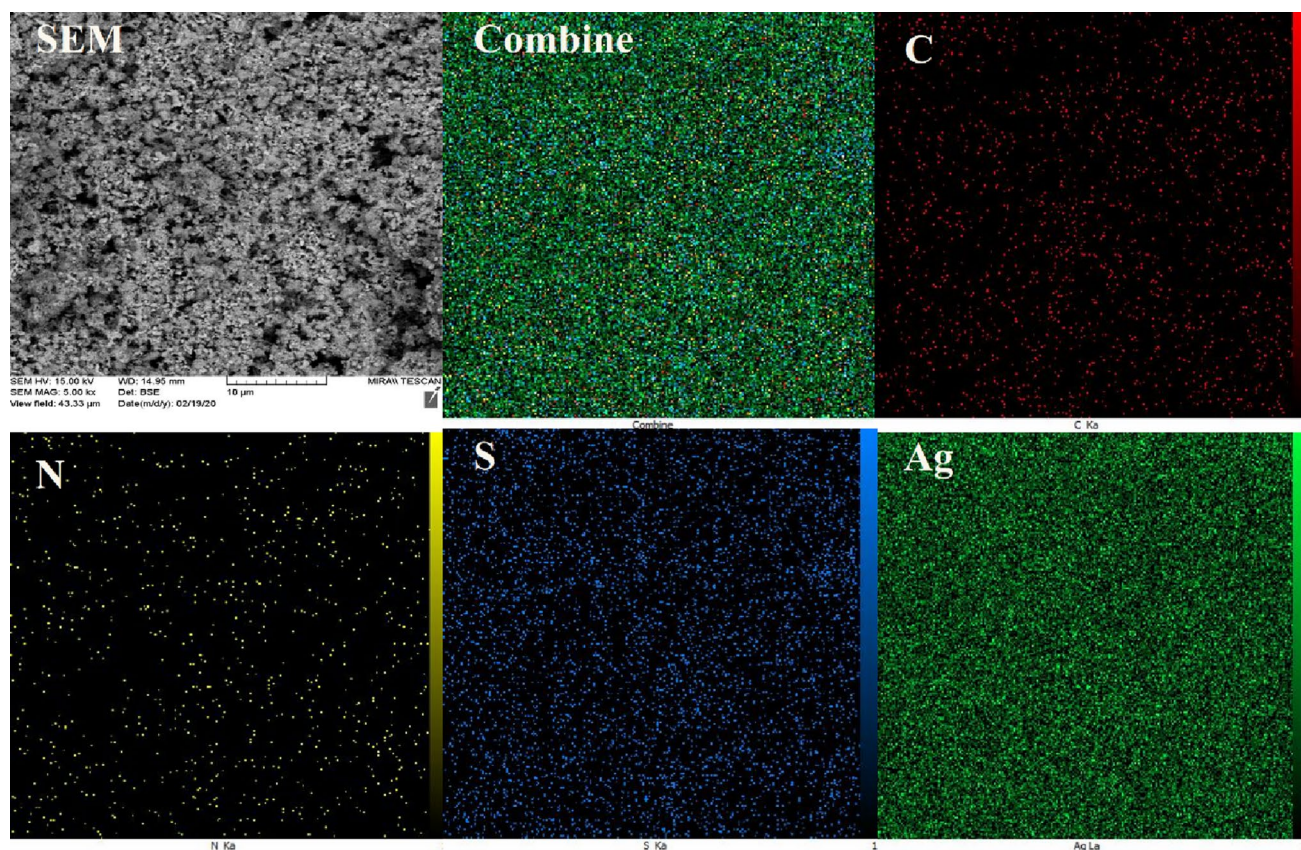


Figure 6. X-ray mapping Analysis of Ag-CP.

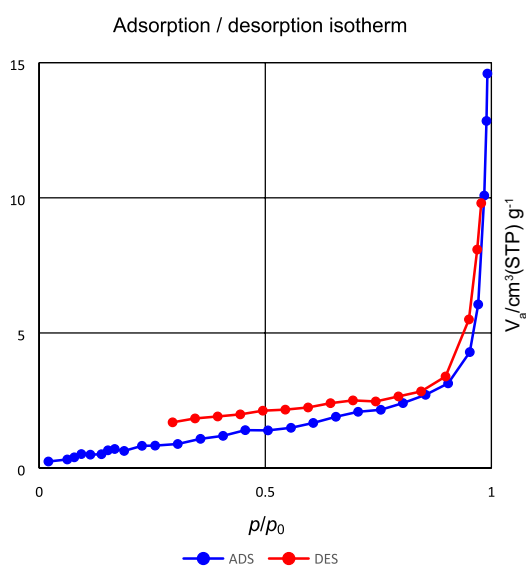
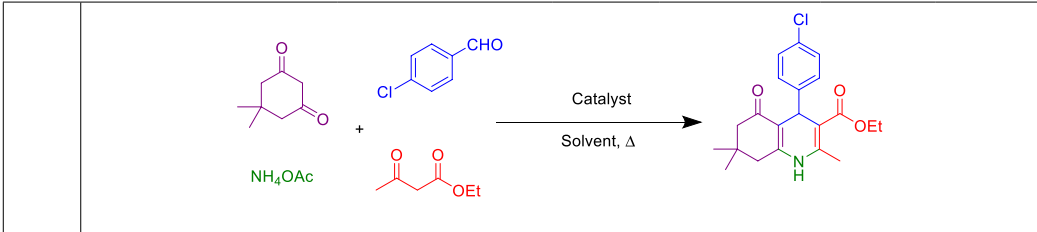


Figure 7. N₂ adsorption/desorption isotherms of the Ag-CP.

entry 10). Subsequently, the effect of different solvents with varying polarity (DMSO, DMF, PEG-400, EtOH and EtOH:H₂O (1:1)) was studied (Table 1, entries 10 and 12–15) and the best reaction yield was carried out in EtOH as solvent. With increasing the temperature from room temperature to 80 °C, a dominant increase in the yield was observed (Table 1, entries 10 and 16–18). Regarding the optimization studies, the optimum conditions for this reaction are: Ag-CP (7 mg) in the EtOH at reflux conditions (Table 1, entry 10). Additionally, the catalytic effect of 4,6-diamino-2-pyrimidinethiol and Ag(NO₃)₂ was investigated on the model reaction. It was observed



Entry	Catalyst	Amount of catalyst (mg)	Solvent	Temperature (°C)	Time (min)	Yield (%) ^{a,b}
1	–	–	EtOH	Reflux	85	17
2	4,6-diamino-2-pyrimidinethiol	7	EtOH	Reflux	85	23
3	Ag(NO ₃) ₂	7	EtOH	Reflux	85	Trace
4	Ag-CP	4	EtOH	Reflux	85	69
5	Ag-CP	5	EtOH	Reflux	85	74
6	Ag-CP	6	EtOH	Reflux	85	78
7	Ag-CP	7	EtOH	Reflux	85	87
8	Ag-CP	7	EtOH:H ₂ O	80	90	82
9	Ag-CP	7	PEG-400	80	120	75
10	Ag-CP	7	DMF	80	110	74
11	Ag-CP	7	DMSO	80	125	78
12	Ag-CP	7	EtOH	25	8 h	NR
13	Ag-CP	7	EtOH	60	70	76
14	Ag-CP	7	EtOH	70	75	79

Table 1. Optimization of the reaction conditions for the Hantzsch condensation of *para*-Chlorobenzaldehyde, dimedone, ethyl acetoacetate and ammonium acetate as a model reaction for the synthesis of polyhydroquinolines. ^aIsolated yield. ^bReaction conditions: 4-Chlorobenzaldehyde (1 mmol), dimedone (1 mmol), ethyl acetoacetate (1 mmol), ammonium acetate (1.2 mmol), catalyst (mg) and solvent (3 mL).

that 4,6-diamino-2-pyrimidinethiol and Ag(NO₃)₂ cannot efficiently catalyze the reaction and, as a result, the product is obtained in low yields in 85 min.

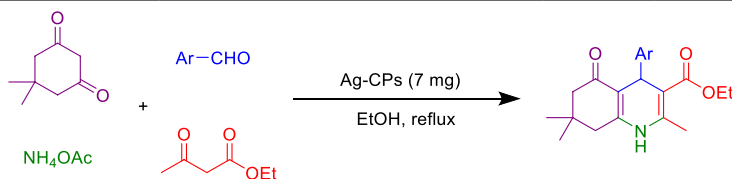
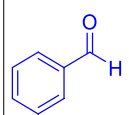
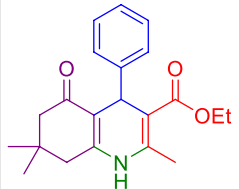
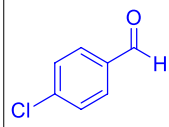
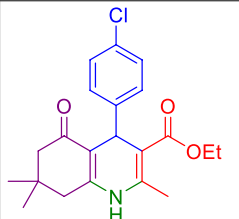
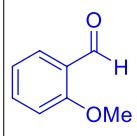
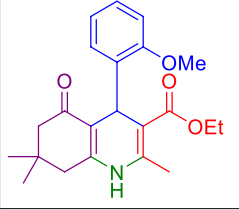
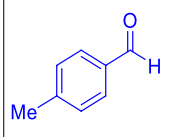
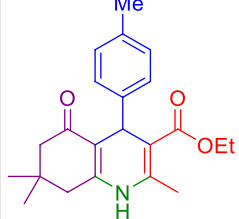
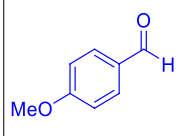
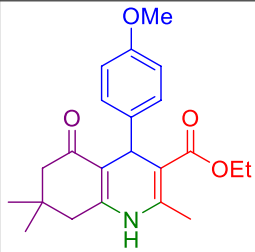
After optimization of the reaction conditions, we have explored the scope of the reaction with various electron-donating and electron-withdrawing groups of aldehydes (Table 2). Both these substituents gave excellent yield of the product.

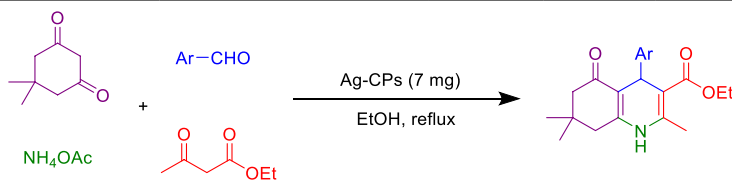
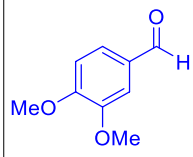
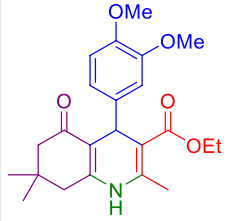
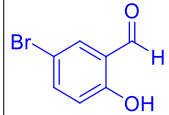
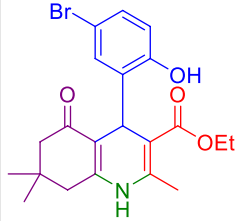
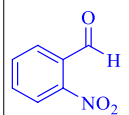
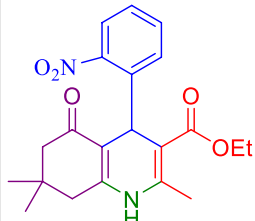
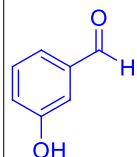
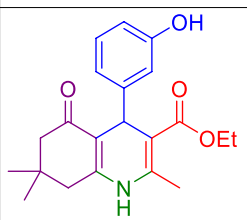
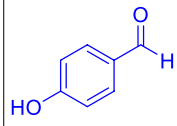
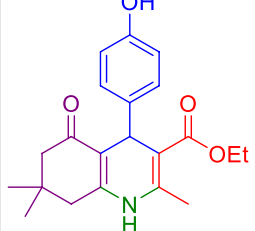
A plausible reaction mechanism for the Hantzsch synthesis of polyhydroquinoline derivatives in the presence of Ag-CP is depicted in Scheme 2. Initially, the carbanion was formed by proton abstraction from the active methylene compounds (ethyl acetoacetate or dimedone) which underwent Knoevenagel condensation reaction with aldehyde to form an α,β -unsaturated compound. In the second part of the reaction, ammonium acetate gave acetic acid and ammonia and, then, the ammonia combined with the active carbonyl compounds (ethyl acetoacetate or dimedone) and attained imine derivatives. Finally, the Michael addition of imine derivatives on the α,β -unsaturated carbonyl compounds (which were activated by Ag-CP) was followed by cyclization reaction. Besides, dehydration gave the final polyhydroquinoline products (Scheme 2).

Hot filtration. The hot filtration test was another analysis to approve the heterogeneous nature of the Ag-CP in the Hantzsch synthesis of polyhydroquinolines. On this basis, the model reaction was studied again under the optimized reaction condition. After 43 min (59% conversion), the Ag-CP were removed from the reaction by simple filtration. Afterwards, the rest of the reaction was stirred in the absence of the catalyst for a further 43 min. The obtained results show that the Ag-based framework played a catalytic role in the reaction without the Ag leaching into the solution or framework degradation.

Recyclability study. Considering the environmental and economic factors, and also the principles of green chemistry, the long-term durability experiment of the prepared catalyst has been investigated. In this sense, the model reaction was carried out under the optimized reaction conditions to test the reusability behaviour of the Ag-CP (Fig. 8). Briefly, after the finalization of each run of the Hantzsch reaction, which was monitored by the thin-layer chromatography, the reaction mixture was cooled to room temperature and, then, the heterogeneous catalyst was separated by simple filtration, washed with Acetone, EtOAc and H₂O and, finally, dried in an oven at 60 °C overnight to be used in the next run. As shown in Fig. 8, no significant decrease in the yield of the reactions was observed even after four runs. These results confirmed the high catalytic activity and long-term durability of the Ag-CP in the Hantzsch synthesis of polyhydroquinolines.

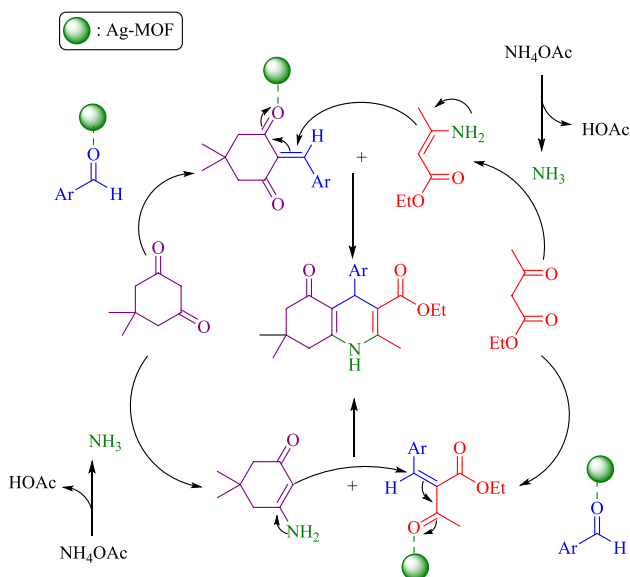
The Ag-CP have been characterized by FT-IR before and after the reaction (Fig. 9a, b). These spectra showed the similar peaks and indicating the stability of this catalyst under applied reaction conditions.

						
Entry	Aryl aldehyde	Product	Time (min)	Yield (%) ^{a,b}	Melting point	
					Measured	Literature
1			80	93	198–205	203–206 ⁶¹
2			85	87	245–248	246–247 ⁶¹
3			80	86	245–249	249–251 ⁶¹
4			86	82	249–251	252–255 ⁴⁷
5			80	83	254–256	255–257 ⁴⁷
Continued						

						
Entry	Aryl aldehyde	Product	Time (min)	Yield (%) ^{a,b}	Melting point	
					Measured	Literature
6			85	87	197–202	204–206 ⁶¹
7			85	88	264–268	246–248 ⁶²
8			80	93	169–174	175–176 ⁶¹
9			80	87	208–210	230–232 ³⁷
10			85	81	238–240	231–233 ⁴⁷
Continued						

Entry	Aryl aldehyde	Product	Time (min)	Yield (%) ^{a,b}	Melting point	
					Measured	Literature
11			85	74	294–295	305–307 ⁶³
12			90	78 ^c	298 ^d	298–300 ⁶⁴

Table 2. Hantzsch synthesis of polyhydroquinoline derivatives in the presence of Ag-CP in EtOH at 80 °C. ^aIsolated yields. ^bReaction conditions: Aromatic aldehyde (1 mmol), dimedone (1 mmol), ethyl acetoacetate (1 mmol), ammonium acetate (1.2 mmol), Ag-CP (7 mg) and EtOH (3 mL) at 80 °C reflux conditions. ^cReaction conditions: Aromatic aldehyde (1 mmol), dimedone (2 mmol), ethyl acetoacetate (2 mmol), ammonium acetate (2.4 mmol), Ag-CP (14 mg) and EtOH (6 mL) at 80 °C reflux conditions. ^dDecomposition.



Scheme 2. Proposed mechanism for the synthesis of polyhydroquinolines in the presence of Ag-CP.

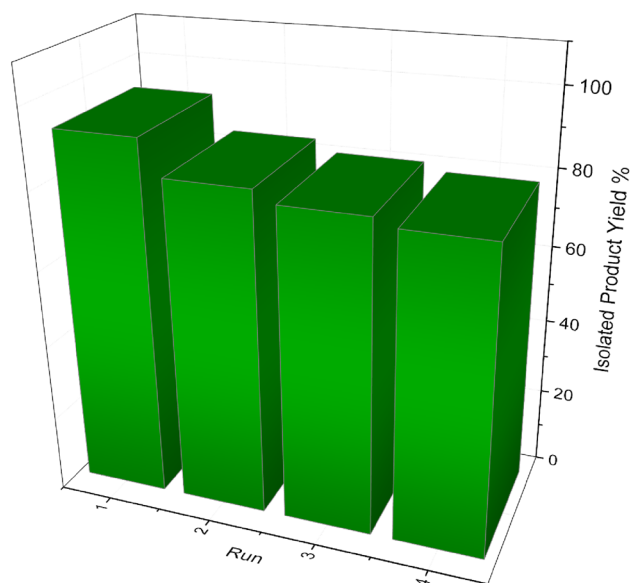


Figure 8. Recyclability of the Ag-CP.

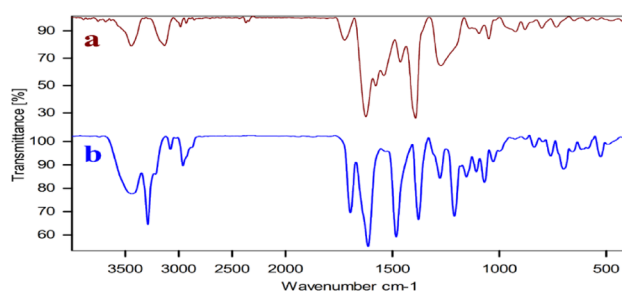


Figure 9. FT-IR spectra of the (a) fresh Ag-CP and (b) spent Ag-CP.

Furthermore, no noticeable changes in crystalline phase can be found from comparison of PXRD of the spent (Fig. 10a) and fresh (Fig. 10b) catalyst. Which shows an excellent physicochemical stability during Hantzsch reaction.

Comparison of the proposed catalyst with the previously reported catalysts for the Hantzsch condensation. Finally, to evaluate the performance of the present catalytic activity in the unsymmetrical Hantzsch reaction, the current protocol was compared with some of the previously reported catalysts in the synthesis of polyhydroquinolines (Table 3). There is no doubt that all of the listed catalysts in Table 3 can significantly produce the desired product in good to excellent yield. But, it was found out that the Ag-CP as a heterogeneous catalyst can be regarded as superior to almost all of the methods presented in Table 3. These observations may be attributed to the synergistic effect between the Ag and the basic sites in the prepared Ag-CP catalytic system.

Conclusion

In summary, a novel Ag-CP catalytic system was successfully prepared using the reaction of 4,6-diamino-2-mercaptopyrimidine which contains a pyrimidine ring, two amine and one thiol functional groups with strong chelating ability and silver nitrate solutions as commercial available starting materials. Besides, it was characterized by a progressive mode for the preparation. The Ag-CP has an efficient catalytic activity for Hantzsch Synthesis of polyhydroquinolines with various aldehyde-bearing aromatic hydrocarbons in green media and in low reaction times. More importantly, the prepared catalyst affords several advantages such as ease of synthesis, wide range of carriers, ligand-free protocol and easy separation. Simultaneously, the catalyst has remarkable stability and recyclability, and the catalytic activity of the Ag-CP without any significant loss of its activity after four times continuous service.

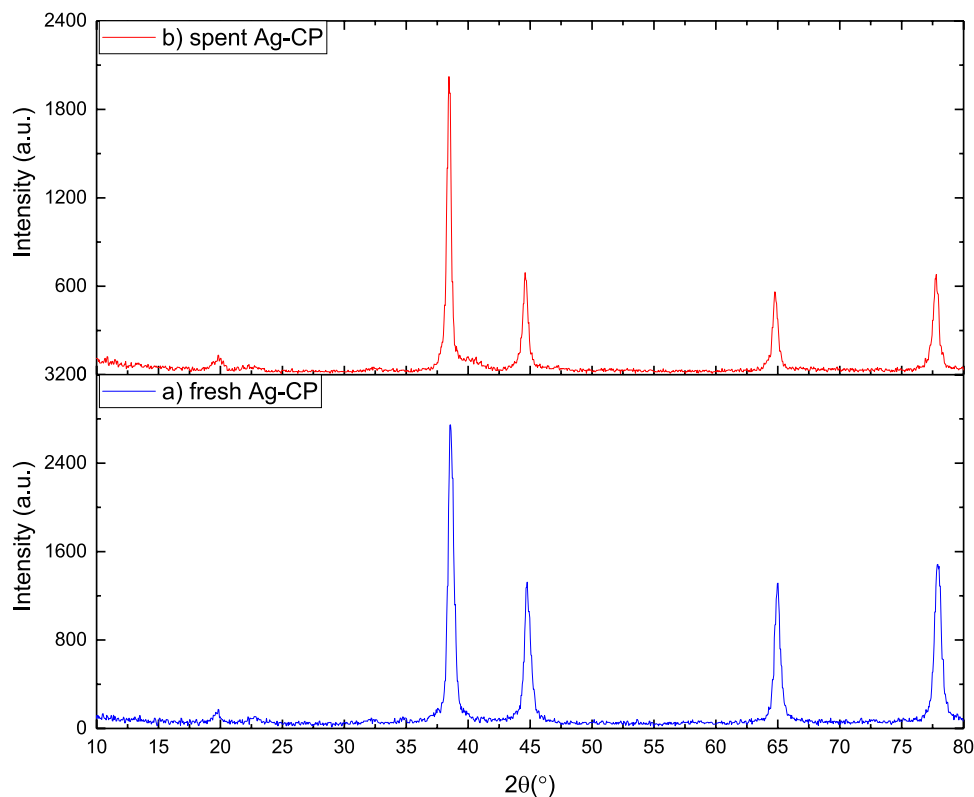


Figure 10. PXRD patterns of the (a) fresh Ag-CP and (b) spent Ag-CP.

Entry	Catalyst	Time (min)	Yield (%) ^a	References
1	FeAl ₂ O ₄	180	90	37
2	Fe ₃ O ₄ @D-NH-(CH ₂) ₄ -SO ₃ H	90	86	65
3	Fe ₃ O ₄ @FSM-16-SO ₃ H	25	86	66
4	AIL-SCMNPs	15	80	67
5	Ag-CP	85	87	This work

Table 3. Comparison of the synthesis of polyhydroquinolines in the presence of various catalysts. ^aIsolated yield.

Received: 22 April 2021; Accepted: 19 July 2021

Published online: 02 August 2021

References

- Li, M., Wu, W. & Jiang, H. Recent advances in silver-catalyzed transformations of electronically unbiased alkenes and alkynes. *ChemCatChem* **12**, 5034–5050 (2020).
- Zhang, J. *et al.* Computational advances aiding mechanistic understanding of silver-catalyzed carbene/nitrene/silylene transfer reactions. *Coord. Chem. Rev.* **382**, 69–84 (2019).
- Sreedevi, R., Saranya, S. & Anilkumar, G. Recent trends in the silver-catalyzed synthesis of nitrogen heterocycles. *Adv. Synth. Catal.* **361**, 4625–4644 (2019).
- Treesa, G. S. S., Saranya, S., Meera, G. & Anilkumar, G. Recent advances and perspectives in the silver-catalyzed multi-component reactions. *Curr. Org. Chem.* **24**, 291–313 (2020).
- Nathaniel, C. R., Neetha, M. & Anilkumar, G. Silver-catalyzed pyrrole synthesis: An overview. *Appl. Organomet. Chem.* <https://doi.org/10.1002/aoc.6141> (2021).
- Olenin, A. Y. & Mingalev, P. G. Similarities and differences in the mechanisms alkyne and isonitrile transformations catalyzed by silver ions and nanoparticles. *Mol. Catal.* **500**, 111258 (2021).
- Mohammadi, M., Khodamorady, M., Tahmasbi, B., Bahrani, K. & Ghorbani-Choghamarani, A. Boehmite nanoparticles as versatile support for organic–inorganic hybrid materials: Synthesis, functionalization, and applications in eco-friendly catalysis. *J. Ind. Eng. Chem.* <https://doi.org/10.1016/j.jiec.2021.02.001> (2021).
- Das, S. K., Chatterjee, S., Mondal, S. & Bhaumik, A. A new triazine-thiophene based porous organic polymer as efficient catalyst for the synthesis of chromenes via multicomponent coupling and catalyst support for facile synthesis of HMF from carbohydrates. *Mol. Catal.* **475**, 110483 (2019).

9. Shao, M., Chang, Q., Dodelet, J. P. & Chenitz, R. Recent advances in electrocatalysts for oxygen reduction reaction. *Chem. Rev.* **116**, 3594–3657 (2016).
10. Ruiz-Castillo, P. & Buchwald, S. L. Applications of palladium-catalyzed C–N cross-coupling reactions. *Chem. Rev.* **116**, 12564–12649 (2016).
11. Bonesi, S. M., Protti, S. & Albini, A. Photochemical co-oxidation of sulfides and phosphines with tris(p-bromophenyl)amine. A mechanistic study. *J. Org. Chem.* **83**, 8104–8113 (2018).
12. Suzuki, T. Organic synthesis involving iridium-catalyzed oxidation. *Chem. Rev.* **111**, 1825–1845 (2011).
13. Kazemi, M. & Mohammadi, M. Magnetically recoverable catalysts: Catalysis in synthesis of polyhydroquinolines. *Appl. Organomet. Chem.* **34**, e5400 (2020).
14. Chetioui, S. *et al.* Cu(II) coordination polymer bearing diazenyl-benzoic ligand: Synthesis, physico-chemical and XRD/HSA-interactions. *J. Mol. Struct.* **1229**, 129604 (2021).
15. Buta, I. *et al.* One-dimensional cadmium(II) coordination polymers: Structural diversity, luminescence and photocatalytic properties. *J. Photochem. Photobiol. A Chem.* **404**, 112961 (2021).
16. Hurlock, M. J., Lare, M. F. & Zhang, Q. Two Cd-based luminescent coordination polymers constructed from a truncated linker. *Inorg. Chem.* <https://doi.org/10.1021/acs.inorgchem.0c03422> (2021).
17. Wei, J. *et al.* Assembly of Zr-based coordination polymer over USY zeolite as a highly efficient and robust acid catalyst for one-pot transformation of fructose into 2,5-bis(isopropoxymethyl)furan. *J. Catal.* **389**, 87–98 (2020).
18. Sakamoto, N. *et al.* Self-assembled cuprous coordination polymer as a catalyst for CO₂ electrochemical reduction into C₂ products. *ACS Catal.* **10**, 10412–10419 (2020).
19. Kulovi, S. *et al.* Polymorphism in [Ag(bpetan)]_n coordination polymers with nitrate and isophthalate anions: Photocatalytic and antibacterial activity, hemolysis assay and study of cytotoxicity. *ChemistrySelect* **5**, 3337–3346 (2020).
20. Kalaj, M. *et al.* MOF-polymer hybrid materials: From simple composites to tailored architectures. *Chem. Rev.* **120**, 8267–8302 (2020).
21. Ding, M., Flaig, R. W., Jiang, H. L. & Yaghi, O. M. Carbon capture and conversion using metal-organic frameworks and MOF-based materials. *Chem. Soc. Rev.* **48**, 2783–2828 (2019).
22. Ghorbani-Choghamarani, A. & Taherinia, Z. Chiral cobalt-peptide metal-organic framework (Co-P-MOF): As an efficient and reusable heterogeneous catalyst for the asymmetric sulfoxidative cross-coupling reaction using poly sulfynylpiperazine. *Synth. Met.* **263**, 116362 (2020).
23. Das, S. K., Mondal, S., Chatterjee, S. & Bhaumik, A. N-rich porous organic polymer as heterogeneous organocatalyst for the one-pot synthesis of polyhydroquinoline derivatives through the Hantzsch condensation reaction. *ChemCatChem* **10**, 2488–2495 (2018).
24. Sorg, J. R., Schäfer, T. C., Schneider, T. & Müller-Buschbaum, K. From a 1D Sb coordination polymer to a 3D Sb framework with pyrazine: Switching off the stereochemically active lone-pair. *Zeitschrift für Anorg. und Allg. Chemie* **646**, 507–513 (2020).
25. Pignaneli, J., Qian, Z., Gu, X., Ahamed, M. J. & Rondeau-Gagné, S. Modulating the thermomechanical properties and self-healing efficiency of siloxane-based soft polymers through metal-ligand coordination. *New J. Chem.* **44**, 8977–8985 (2020).
26. Kuwahara, T., Ohtsu, H. & Tsuge, K. Synthesis and photophysical properties of emissive silver(I) halogenido coordination polymers composed of Ag₂X₂ units bridged by pyrazine, methylpyrazine, and aminopyrazine. *Inorg. Chem.* **60**, 1299–1304 (2021).
27. Nana, A. N. *et al.* Nanochanneled silver-deficient tris(oxalato)chromate(III) coordination polymers: Synthesis, crystal structure, spectroscopy, thermal analysis and magnetism. *J. Mol. Struct.* **1220**, 128642 (2020).
28. Ristić, P. *et al.* 1D and 2D silver-based coordination polymers with thiomorpholine-4-carbonitrile and aromatic polyoxoacids as coligands: Structure, photocatalysis, photoluminescence, and TD-DFT study. *Cryst. Growth Des.* **20**, 4461–4478 (2020).
29. Pal, A. *et al.* A phosphate-based silver-bipyridine 1D coordination polymer with crystallized phosphoric acid as superprotonic conductor. *Chem.—A Eur. J.* **26**, 4607–4612 (2020).
30. Mondal, S., Patra, B. C. & Bhaumik, A. One-pot synthesis of polyhydroquinoline derivatives through organic-solid-acid-catalyzed Hantzsch condensation reaction. *ChemCatChem* **9**, 1469–1475 (2017).
31. Zhang, Y. *et al.* Robust bifunctional lanthanide cluster based metal-organic frameworks (MOFs) for tandem deacetalization–Knoevenagel reaction. *Inorg. Chem.* **57**, 2193–2198 (2018).
32. Zhao, S.-Y., Chen, Z.-Y., Wei, N., Liu, L. & Han, Z.-B. Highly efficient cooperative catalysis of single-site Lewis acid and Brønsted acid in a metal-organic framework for the Biginelli reaction. *Inorg. Chem.* **58**, 7657–7661 (2019).
33. Cankařová, N. & Krchňák, V. Isocyanide multicomponent reactions on solid phase: State of the art and future application. *Int. J. Mol. Sci.* **21**, 1–48 (2020).
34. Innocenti, R., Lenci, E. & Trabocchi, A. Recent advances in copper-catalyzed imine-based multicomponent reactions. *Tetrahedron Lett.* **61**, 152083 (2020).
35. Lei, J. *et al.* An acid-catalyzed 1,4-addition isocyanide-based multicomponent reaction in neat water. *Green Chem.* **22**, 3716–3720 (2020).
36. Serafini, M., Murgia, I., Giustiniano, M., Pirali, T. & Tron, G. C. The 115 year old multicomponent Bargellini reaction: Perspectives and new applications. *Molecules* **26**, 558 (2021).
37. Ghorbani-Choghamarani, A., Mohammadi, M., Shiri, L. & Taherinia, Z. Synthesis and characterization of spinel FeAl₂O₄ (hercynite) magnetic nanoparticles and their application in multicomponent reactions. *Res. Chem. Intermed.* **45**, 5705–5723 (2019).
38. Nikoorazm, M., Mohammadi, M. & Khanmoradi, M. Zirconium@guanine@MCM-41 nanoparticles: An efficient heterogeneous mesoporous nanocatalyst for one-pot, multi-component tandem Knoevenagel condensation–Michael addition–cyclization reactions. *Appl. Organomet. Chem.* **34**, e5704 (2020).
39. Nikoorazm, M., Khanmoradi, M. & Mohammadi, M. Guanine-La complex supported onto SBA-15: A novel efficient heterogeneous mesoporous nanocatalyst for one-pot, multi-component tandem Knoevenagel condensation–Michael addition–cyclization reactions. *Appl. Organomet. Chem.* **34**, e5504 (2020).
40. Zhang, W., Zhi, S. & Ma, X. Consecutive multicomponent reactions for the synthesis of complex molecules. *Org. Biomol. Chem.* **17**, 7632–7650 (2019).
41. Cimarelli, C. Multicomponent reactions. *Molecules* **24**, 2372 (2019).
42. Schaper, K. & Müller, T. J. J. Thiophene syntheses by ring forming multicomponent reactions. *Top. Curr. Chem.* **376**, 261–283 (2018).
43. Nope, E. *et al.* Hydrotalcites in organic synthesis: Multicomponent reactions. *Curr. Org. Synth.* **15**, 1073–1090 (2018).
44. Esam, Z., Akhavan, M., Bekhradnia, A., Mohammadi, M. & Tourani, S. A novel magnetic immobilized para-aminobenzoic acid-Cu(II) complex: A green, efficient and reusable catalyst for aldol condensation reactions in green media. *Catal. Lett.* **150**, 3112–3131 (2020).
45. Tamoradi, T., Mousavi, S. M. & Mohammadi, M. Synthesis of a new Ni complex supported on CoFe₂O₄ and its application as an efficient and green catalyst for the synthesis of bis(pyrazolyl)methane and polyhydroquinoline derivatives. *New J. Chem.* **44**, 8289–8302 (2020).
46. Tamoradi, T., Mousavi, S. M. & Mohammadi, M. Praseodymium(III) anchored on CoFe₂O₄ MNPs: an efficient heterogeneous magnetic nanocatalyst for one-pot, multi-component domino synthesis of polyhydroquinoline and 2,3-dihydroquinazolin-4(1H)-one derivatives. *New J. Chem.* **44**, 3012–3020 (2020).

47. Ghorbani-Choghamarani, A., Mohammadi, M., Tamoradi, T. & Ghadermazi, M. Covalent immobilization of Co complex on the surface of SBA-15: Green, novel and efficient catalyst for the oxidation of sulfides and synthesis of polyhydroquinoline derivatives in green condition. *Polyhedron* **158**, 25–35 (2019).
48. Rathod, V. N., Bansode, N. D., Thombre, P. B. & Lande, M. K. Efficient one-pot synthesis of polyhydroquinoline derivatives through the Hantzsch condensation using IRMOF-3 as heterogeneous and reusable catalyst. *J. Chin. Chem. Soc.* <https://doi.org/10.1002/jccs.202000303> (2021).
49. Khodabakhshi, M. R., Kiamehr, M. & Karimian, R. Efficient one-pot synthesis of 1,4-dihydropyridine and polyhydroquinoline derivatives using sulfanilic acid-functionalized boehmite nano-particles as an organic-inorganic hybrid catalyst. *Polycycl. Aromat. Compd.* <https://doi.org/10.1080/10406638.2021.1884100> (2021).
50. Roozifar, M., Hazeri, N. & Faroughi Niya, H. Application of salicylic acid as an eco-friendly and efficient catalyst for the synthesis of 2,4,6-triaryl pyridine, 2-amino-3-cyanopyridine, and polyhydroquinoline derivatives. *J. Heterocycl. Chem.* <https://doi.org/10.1002/jhet.4242> (2021).
51. Nguyen, V. T., Nguyen, H. T. & Tran, P. H. One-pot three-component synthesis of 1-amidoalkyl naphthols and polyhydroquinolines using a deep eutectic solvent: A green method and mechanistic insight. *New J. Chem.* **45**, 2053–2059 (2021).
52. Farsi, R., Mohammadi, M. K. & Saghanezhad, S. J. Sulfonamide-functionalized covalent organic framework (COF-SO₃H): an efficient heterogeneous acidic catalyst for the one-pot preparation of polyhydroquinoline and 1,4-dihydropyridine derivatives. *Res. Chem. Intermed.* **47**, 1161–1179 (2021).
53. Sharma, S., Singh, U. P. & Singh, A. P. Synthesis of MCM-41 supported cobalt (II) complex for the formation of polyhydroquinoline derivatives. *Polyhedron* **199**, 115102 (2021).
54. Guo, H., Zhang, Y., Zheng, Z., Lin, H. & Zhang, Y. Facile one-pot fabrication of Ag@MOF(Ag) nanocomposites for highly selective detection of 2,4,6-trinitrophenol in aqueous phase. *Talanta* **170**, 146–151 (2017).
55. Lajevardi, A., Yarak, M. T., Masjedi, A., Nouri, A. & Sadr, M. H. Green synthesis of MOF@Ag nanocomposites for catalytic reduction of methylene blue. *J. Mol. Liq.* **276**, 371–378 (2019).
56. Maleki, B., Reiser, O., Esmailnezhad, E. & Choi, H. J. SO₃H-dendrimer functionalized magnetic nanoparticles (Fe₃O₄@D-NH-(CH₂)₄-SO₃H): Synthesis, characterization and its application as a novel and heterogeneous catalyst for the one-pot synthesis of polyfunctionalized pyrans and polyhydroquinolines. *Polyhedron* **162**, 129–141 (2019).
57. Moradi, L. & Tadayan, M. Green synthesis of 3,4-dihydropyrimidinones using nano Fe₃O₄@meglumine sulfonic acid as a new efficient solid acid catalyst under microwave irradiation. *J. Saudi Chem. Soc.* **22**, 66–75 (2018).
58. Ahmadi, A., Sedaghat, T., Azadi, R. & Motamedi, H. Magnetic mesoporous silica nanocomposite functionalized with palladium Schiff base complex: Synthesis, characterization, catalytic efficacy in the Suzuki-Miyaura reaction and α-amylase immobilization. *Catal. Lett.* **150**, 112–126 (2020).
59. Li, Y.-Y., Wang, F.-R., Li, Z.-Y., Yan, Z.-N. & Niu, Y.-Y. Assembly and adsorption properties of seven supramolecular compounds with heteromacrocyclic imidazolium. *ACS Omega* **4**, 8926–8934 (2019).
60. Alheety, M. A. *et al.* Ag(I)-benzisothiazolinone complex: Synthesis, characterization, H₂ storage ability, nano transformation to different Ag nanostructures and Ag nanoflakes antimicrobial activity. *Mater. Res. Express* **6**, 125071 (2019).
61. Nikoorazm, M. & Erfani, Z. Core-shell nanostructure (Fe₃O₄@MCM-41@Cu-P2C) as a highly efficient and recoverable nanocatalyst for the synthesis of polyhydroquinoline, 5-substituted 1H-tetrazoles and sulfides. *Chem. Phys. Lett.* **737**, 136784 (2019).
62. Amoozadeh, A., Rahmani, S., Bitaraf, M., Abadi, F. B. & Tabrizian, E. Nano-zirconia as an excellent nano support for immobilization of sulfonic acid: A new, efficient and highly recyclable heterogeneous solid acid nanocatalyst for multicomponent reactions. *New J. Chem.* **40**, 770–780 (2016).
63. Goli-Jolodar, O., Shirini, F. & Seddighi, M. Introduction of a novel nanosized N-sulfonated Brønsted acidic catalyst for the promotion of the synthesis of polyhydroquinoline derivatives via Hantzsch condensation under solvent-free conditions. *RSC Adv.* **6**, 26026–26037 (2016).
64. Abedini, M., Shirini, F. & Mousapour, M. Poly(vinylpyrrolidinium) perchlorate as a new and efficient catalyst for the promotion of the synthesis of polyhydroquinoline derivatives via Hantzsch condensation. *Res. Chem. Intermed.* **42**, 2303–2315 (2016).
65. Alinezhad, H., Tarahomi, M., Maleki, B. & Amiri, A. SO₃H-functionalized nano-MGO-D-NH₂: Synthesis, characterization and application for one-pot synthesis of pyrano[2,3-d]pyrimidinone and tetrahydrobenzo[b]pyran derivatives in aqueous media. *Appl. Organomet. Chem.* **33**, e4661 (2019).
66. Hashemi-Uderji, S., Abdollahi-Alibeik, M. & Ranjbar-Karimi, R. Fe₃O₄@FSM-16-SO₃H as a novel magnetically recoverable nanostructured catalyst: Preparation, characterization and catalytic application. *J. Porous Mater.* **26**, 467–480 (2019).
67. Taheri, N., Heidarizadeh, F. & Kiasat, A. A new magnetically recoverable catalyst promoting the synthesis of 1,4-dihydropyridine and polyhydroquinoline derivatives via the Hantzsch condensation under solvent-free conditions. *J. Magn. Magn. Mater.* **428**, 481–487 (2017).

Acknowledgements

This work was supported by the research facilities of Ilam University, Ilam, Iran, and Bu-Ali Sina University, Hamedan, Iran.

Author contributions

N.H.-K. did the experimental works. A.G.-C. supervised the research project and is the corresponding author of the manuscript. M.M. write the manuscript draft.

Competing interests

The authors declare no competing interests.

Additional information

Correspondence and requests for materials should be addressed to A.G.-C.

Reprints and permissions information is available at www.nature.com/reprints.

Publisher's note Springer Nature remains neutral with regard to jurisdictional claims in published maps and institutional affiliations.



Open Access This article is licensed under a Creative Commons Attribution 4.0 International License, which permits use, sharing, adaptation, distribution and reproduction in any medium or format, as long as you give appropriate credit to the original author(s) and the source, provide a link to the Creative Commons licence, and indicate if changes were made. The images or other third party material in this article are included in the article's Creative Commons licence, unless indicated otherwise in a credit line to the material. If material is not included in the article's Creative Commons licence and your intended use is not permitted by statutory regulation or exceeds the permitted use, you will need to obtain permission directly from the copyright holder. To view a copy of this licence, visit <http://creativecommons.org/licenses/by/4.0/>.

© The Author(s) 2021